

re-submitted to ApJ, on August 23, 2018

A general relativistic model of accretion disks with coronae surrounding Kerr black holes

Bei You¹, Xinwu Cao¹, and Ye-Fei Yuan²

ABSTRACT

We calculate the structure of a standard accretion disk with corona surrounding a massive Kerr black hole in general relativistic frame, in which the corona is assumed to be heated by the reconnection of the strongly buoyant magnetic fields generated in the cold accretion disk. The emergent spectra of the accretion disk-corona systems are calculated by using the relativistic ray-tracing method. We propose a new method to calculate the emergent Comptonized spectra from the coronae. The spectra of the disk-corona systems with a modified α -magnetic stress show that both the hard X-ray spectral index and the hard X-ray bolometric correction factor $L_{\text{bol}}/L_{X,2-10\text{keV}}$ increase with the dimensionless mass accretion rate, which are qualitatively consistent with the observations of active galactic nuclei (AGNs). The fraction of the power dissipated in the corona decreases with increasing black hole spin parameter a , which leads to lower electron temperatures of the coronas for rapidly spinning black holes. The X-ray emission from the coronas surrounding rapidly spinning black holes becomes weak and soft. The ratio of the X-ray luminosity to the optical/UV luminosity increases with the viewing angle, while the spectral shape in the X-ray band is insensitive with the viewing angle. We find that the spectral index in the infrared waveband depends on the mass accretion rate and the black hole spin a , which deviates from $f_\nu \propto \nu^{1/3}$ expected by the standard thin disk model.

Subject headings: accretion, accretion disks, black hole physics, magnetic fields, galaxies: active

¹Key Laboratory for Research in Galaxies and Cosmology, Shanghai Astronomical Observatory, Chinese Academy of Sciences, 80 Nandan Road, Shanghai, 200030, China; youbei@shao.ac.cn, cxw@shao.ac.cn

²Department of Astronomy, University of Sciences and Technology of China, Hefei, Anhui 230026, China; yfyuan@ustc.edu.cn

1. Introduction

Active galactic nuclei (AGNs) are powered by the accretion of gases on to their central massive black holes, and the emission of the accretion disks is responsible for the observed multi-band spectral energy distributions (SEDs). It is suggested that the optically thick and geometrically thin accretion disks are present in luminous AGNs, and the observed UV/optical continuum emission of AGNs is the thermal emission from the standard thin accretion disks (e.g., Shakura & Sunyaev 1973; Shields 1978; Malkan & Sargent 1982; Sun & Malkan 1989; Laor & Netzer 1989; Laor 1990; Czerny et al. 2011; Hu & Zhang 2012). One feature in the spectra of such standard thin accretion disks surrounding massive black holes is, $f_\nu \propto \nu^{1/3}$, in the infrared waveband (Koratkar & Blaes 1999). As the accretion disk extends to the region very close to the black hole, the general relativistic thin accretion disk models were developed in the previous works (e.g., Novikov & Thorne 1973; Page & Thorne 1974; Laor & Netzer 1989; Li et al. 2005; Abramowicz & Fragile 2011), which were applied successfully to fit the observed SEDs of AGNs and the values of black hole spin parameter can be derived for some sources (e.g., Laor 1990; Czerny et al. 2011). The values of the spin parameter were estimated by the comparison of the theoretical accretion disk spectra with the observed spectra in some X-ray binaries (Zhang et al. 1997; Steiner et al. 2009; Gou et al. 2011; Kulkarni et al. 2011; McClintock et al. 2011). However, the temperature of the standard thin accretion disks is too low to produce the observed power-law spectra of AGNs in the hard X-ray waveband, and the accretion disk-corona model was therefore suggested (e.g., Galeev et al. 1979; Haardt & Maraschi 1991; Svensson & Zdziarski 1994). In this scenario, the power-law hard X-ray spectra of AGNs are most likely due to the inverse Compton scattering of soft photons on a population of hot electrons in the corona above the disk. The soft photons are emitted from the cold disk, and most of them pass through the optically thin corona without being scattered, which emerge as the observed optical/UV continuum emission of AGNs. A small fraction of the photons from the cold disk are Compton scattered by the hot electrons in the corona to the hard X-ray energy band. The disk-corona model was extensively explored in many previous works (e.g., Haardt & Maraschi 1991; Svensson & Zdziarski 1994; Kawaguchi et al. 2001; Liu et al. 2002; Cao 2009). Most gravitational energy is generated in the cold disk through the turbulence, which is probably produced by the magnetorotational instability (Balbus & Hawley 1991). A fraction of the energy generated in the cold disk should be transported to the corona. One of the most promising mechanisms is the energy of the strongly buoyant magnetic fields in the disk being transported vertically to heat the corona above the disk with the reconnection of the fields (e.g. Di Matteo 1998; Di Matteo et al. 1999; Merloni & Fabian 2001). The temperature of the hot electrons in the corona is roughly around 10^9 K, which can successfully reproduce a power-law hard X-ray spectrum as observed in AGNs (e.g. Liu et al. 2003; Cao 2009).

The emergent spectrum of an accretion disk surrounding a rotating black hole is influenced by the relativistic effects due to the strong gravity field of the hole, which was extensively investigated in many works (e.g., Zhang et al. 1985; Laor & Netzer 1989; Laor 1991; Li et al. 2005, 2009). The iron $K\alpha$ fluorescence lines observed in some AGNs are significantly asymmetric, characterized with a steep blue wing, an extended red wing and the blueshifted emission line peak (see Miller 2007, for a review, and the references therein). These features can be modeled as emission from the inner region of an accretion disk illuminated by the external X-ray radiation with the Doppler boost effect and the general relativistic effects (frame-dragging, gravitational redshift and bending of the light) being properly considered (e.g., Laor 1991). Such effects should also be considered in the calculations of the emergent continuum spectrum of an accretion disk surrounding a rotating black hole observed at infinity (e.g., Laor & Netzer 1989; Zhang et al. 1997; Laor 1991; Li et al. 2005, 2009). The ray-tracing method is widely adopted to derive the photon trajectories bent by the strong gravity field of the black hole in the calculations of the emergent spectra emitted from the disk (e.g., Chandrasekhar 1983; Rauch & Blandford 1994; Cadez et al. 1998; Fuerst & Wu 2004; Yuan et al. 2009; Abramowicz & Fragile 2011). The values of black hole spin parameter can be estimated by the comparison of the observed spectra with the theoretical model calculations (e.g., Yuan et al. 2010). Besides the radiation from the disk, the emergent spectrum of the corona is also affected by these general relativistic effects, which is more complicated than the disk case due to the complexity of the radiation transfer of Comptonized photons in the geometrically thick corona (e.g., Schnittman & Krolik 2010).

In this work, we calculate the structure of a thin accretion disk with corona surrounding a massive Kerr black hole in general relativistic frame, in which the corona is assumed to be heated by the reconnection of the magnetic fields generated by buoyancy instability in the cold accretion disk. The emergent spectra of the accretion disk-corona systems are calculated by using the relativistic ray-tracing method. The emergent Comptonized spectra from the coronae are calculated by dividing layers in the coronae. We summarize the calculations of the disk-corona structure and its emergent spectrum in Sections 2-4. The numerical results of the model calculations and the discussion are given in Sections 5 and 6.

2. The accretion disk-corona structure

In the Boyer-Lindquist coordinates (t, r, θ, ϕ) with natural units $G = c = 1$, the Kerr metric is

$$ds^2 = -e^{2\nu} dt^2 + e^{2\psi} (d\phi - \omega dt)^2 + e^{2\mu_1} dr^2 + e^{2\mu_2} d\theta^2 \quad (1)$$

where

$$e^{2\nu} = \frac{\Sigma\Delta}{\xi}, \quad e^{2\psi} = \frac{\xi \sin^2 \theta}{\Sigma}, \quad e^{2\mu_1} = \frac{\Sigma}{\Delta}, \quad e^{2\mu_2} = \Sigma, \quad \omega = \frac{2M_{\text{bh}}ar}{\xi},$$

$$\Delta = r^2 - 2M_{\text{bh}}r + a^2, \quad \Sigma = r^2 + a^2 \cos^2 \theta, \quad \xi = (r^2 + a^2)^2 - a^2\Delta \sin^2 \theta, \quad (2)$$

M_{bh} is the mass of black hole, and a is the black hole spin parameter ($-1 \leq a \leq 1$). The event horizon of the black hole is

$$r_+ = M_{\text{bh}} + (M_{\text{bh}}^2 - a^2)^{1/2}. \quad (3)$$

The Keplerian velocity of the matter moving around the black hole in circular orbits in the equatorial plane at radius R is given by

$$\Omega_{\text{K}} = \pm \frac{M_{\text{bh}}^{1/2}}{R^{3/2} \pm aM_{\text{bh}}^{1/2}}, \quad (4)$$

where the upper sign refers to direct orbits, i.e., corotating with the black hole spinning direction, and the lower sign refers to retrograde orbits, i.e., counterrotating with the black hole spinning direction. The innermost of a geometrically thin accretion disk is assumed to extend to the marginally stable circular orbit of the black hole, which is given by

$$r_{\text{ms}} = M_{\text{bh}} \{3 + Z_2 \mp [(3 - Z_1)(3 + Z_1 + 2Z_2)]^{1/2}\}, \quad (5)$$

where

$$Z_1 = 1 + \left(1 - \frac{a^2}{M_{\text{bh}}^2}\right)^{1/3} \left[\left(1 + \frac{a}{M_{\text{bh}}}\right)^{1/3} + \left(1 - \frac{a}{M_{\text{bh}}}\right)^{1/3} \right],$$

and

$$Z_2 = \left(\frac{3a^2}{M_{\text{bh}}^2} + Z_1^2\right)^{1/2}.$$

In this work, we consider the relativistic accretion disk with corona, in which the cold disk is optically thick and geometrically thin. The circular motion of the matter in the accretion disk is assumed to be Keplerian, as that in the standard thin disk model (Shakura & Sunyaev 1973). The formulation of the relativistic accretion disk model is similar to the standard thin disk model, in which some general relativistic correction factors A , B , C , D , and L , are included (Novikov & Thorne 1973; Page & Thorne 1974). The values of all these quantities approach unity in the region far from the black hole (see Abramowicz & Fragile 2011, for a review).

The gravitational power of the matter dissipated in unit surface area of the accretion disk is

$$Q_{\text{dissi}}^+ = \frac{3GM_{\text{bh}}\dot{M}}{8\pi R^3} \frac{L}{BC^{1/2}}, \quad (6)$$

where \dot{M} is the mass accretion rate of the disk. A fraction of the dissipated power is transported to the corona most probably by the magnetic fields generated in the disk. The fields are strongly buoyant, and the corona above the disk is heated with the reconnection of the magnetic fields (Di Matteo 1998). The soft photons emitted from the disk are Compton scattered by the hot electrons in the corona to high energy, which is the main cooling process in the corona. About half of the scattered photons are intercepted by the disk, part of which are reflected and the remainder are re-radiated as blackbody radiation (Zdziarski et al. 1999). Thus, the energy equation for the cold disk is

$$Q_{\text{dissi}}^+ - Q_{\text{cor}}^+ + \frac{1}{2}(1 - f)Q_{\text{cor}}^+ = \frac{4\sigma T_{\text{d}}^4}{3\tau} \quad (7)$$

where T_{d} is the interior temperature in the mid-plane of the disk, and $\tau = \tau_{\text{es}} + \tau_{\text{ff}}$ is the optical depth in the vertical direction of the disk, and the reflection albedo $f = 0.15$ is adopted in all our calculations. The power transported from the disk to the corona is (Di Matteo 1998)

$$Q_{\text{cor}}^+ = p_{\text{m}}v_{\text{p}} = \frac{B^2}{8\pi}v_{\text{p}} \quad (8)$$

where p_{m} is the magnetic pressure in the disk, and v_{p} is the vertically rising speed of the magnetic fields in the accretion disk. The rising speed v_{p} is assumed to be proportional to internal Alfvén velocity, i.e., $v_{\text{p}} = bv_{\text{A}}$, in which b is of the order of unity for extremely evacuated magnetic loops. The strength of the magnetic fields in the disk is crucial in our present investigation, which determines the ratio of power dissipated in the corona to that in the disk. This ratio can be constrained by the observed ratio of the X-ray to bolometric luminosities, which seems to support that the values of b should not deviate significantly from unity in most AGNs, though a low value of b (e.g. $b \lesssim 0.1$) cannot be ruled out in few individual AGNs with extremely low $L_{\text{X}}/L_{\text{bol}}$ (see Vasudevan & Fabian 2007; Cao 2009). The detailed physics for generating magnetic fields in the accretion disks is still quite unclear, and we assume the magnetic stress tensor to be related to the pressure of the disk, as done in many previous works (e.g., Sakimoto & Coroniti 1981; Stella & Rosner 1984; Taam & Lin 1984; Hirose et al. 2009). Cao (2009) constructed accretion disk-corona models with different magnetic stress tensors, and found that the model calculations can qualitatively reproduce the observational features that both the hard X-ray spectral index and the hard X-ray bolometric correction factor $L_{\text{bol}}/L_{\text{X},2-10\text{keV}}$ increase with the Eddington ratio, if $\tau_{r\phi} = p_{\text{m}} = \alpha\sqrt{p_{\text{gas}}p_{\text{tot}}}$ ($p_{\text{tot}} = p_{\text{gas}} + p_{\text{rad}}$ is adopted). We use this magnetic stress tensor in most of our calculations in this work.

The angular momentum equation for the gas in the disk is (Novikov & Thorne 1973)

$$4\pi H_{\text{d}}\tau_{r\phi} = \dot{M}\sqrt{\frac{GM_{\text{bh}}}{R^3}}\frac{F}{D}, \quad (9)$$

where H_d is the scale height of the accretion disk and the factor F is first introduced in Riffert & Herold (1995) in the form of a function D . In the vertical direction of the accretion disk, the hydrostatic equilibrium is assumed. The vertical pressure gradient being balanced with the vertical component of the gravity leads to (Riffert & Herold 1995; McClintock et al. 2006)

$$\frac{dp}{dz} = -\frac{\rho GM_{\text{bh}} z J}{R^3 C} \quad (10)$$

which is valid for the geometrically thin disk, and $J = 1 - \frac{4a}{r^{3/2}} + \frac{3a^2}{r^2}$. Thus the scale height of the disk is given by

$$H_d = c_s \left(\frac{R^3 C}{GM_{\text{bh}} J} \right)^{1/2}, \quad (11)$$

where the sound speed $c_s = [(p_{\text{tot}} + p_m)/\rho]^{1/2}$.

The continuity equation of the disk is

$$\dot{M} = -4\pi R H_d \rho V_r D^{1/2}, \quad (12)$$

where $\rho(R)$ is the mean density of the disk, $V_r(R)$ is the radial velocity of the accretion flow at radius R , and the mass accreted in the corona is neglected.

The state equation of the gas in the disk is

$$p_{\text{tot}} = p_{\text{gas}} + p_{\text{rad}} = \frac{\rho k T_d}{\mu m_p} + \frac{1}{3} a_0 T_d^4 \quad (13)$$

where a_0 is the radiation constant, the mean atomic mass $\mu = (1/\mu_i + 1/\mu_e)^{-1}$. We assume the plasma to consist of 3/4 hydrogen and 1/4 helium, i.e., $\mu_i = 1.23$ and $\mu_e = 1.14$.

The ions and electrons in the corona are heated by the reconnection of the magnetic fields rising from the disk, of which the cooling is dominated by the inverse Compton scattering of the soft photons from the disk, the synchrotron radiation, and the bremsstrahlung radiation. The energy equation of the two-temperature corona is given by (Di Matteo 1998)

$$Q_{\text{cor}}^+ = Q_{\text{cor}}^{\text{ie}} + \delta Q_{\text{cor}}^+ = F_{\text{cor}}^-, \quad (14)$$

where $F_{\text{cor}}^- = F_{\text{syn}}^- + F_{\text{brem}}^- + F_{\text{comp}}^-$ is the cooling rate in unit surface area of the corona, and $Q_{\text{cor}}^{\text{ie}}$ is the energy transfer rate from the ions to the electrons in the corona via Coulomb collisions, which is given by Stepney & Guilbert (1983). We adopt the fraction of the energy directly heating the electrons $\delta = 0.5$ in all our calculations (Bisnovaty-Kogan & Lovelace 1997, 2000). The cooling terms F_{syn}^- and F_{brem}^- are the functions of the magnetic field strength, the number density and temperature of the electrons in the corona, which are taken from

Narayan & Yi (1995). The cooling rate F_{Compt}^- of the Compton scattering in the corona is calculated by using the approach suggested by Coppi & Blandford (1990).

The state equation of the gas in the optically thin corona is

$$p_{\text{cor}} = \frac{\rho_{\text{cor}} k T_i}{\mu_i m_p} + \frac{\rho_{\text{cor}} k T_e}{\mu_e m_p} + p_{\text{cor,m}}, \quad (15)$$

where T_i and T_e are the temperatures of the ions and electrons in the two-temperature corona, and the magnetic pressure $p_{\text{cor,m}} = B_{\text{cor}}^2/8\pi$. Given uncertainty of the magnetic fields in the corona, we simply assume the magnetic pressure to be equipartition with the gas pressure in the corona (Cao 2009). The cooling of the corona is always dominated by the inverse Compton scattering, and the strength of the fields in the corona mainly affects the synchrotron radiation. Our final results are almost independent of the value of the field strength adopted, except for the spectra in radio wavebands. The scale height of the corona H_{cor} can be estimated based on the assumption of static hydrodynamical equilibrium in the vertical direction.

As done in the work of Cao (2009), we need to specify the ion temperature of the corona in the calculations of the disk-corona structure. It is found that the ion temperature T_i has little influence on the X-ray spectra, and Liu et al. (2003) pointed out that the temperature of the ions in the corona is always in the range of ~ 0.2 - 0.3 virial temperature ($T_{\text{vir}} = GM_{\text{bh}}m_p/kR$). In this work, the definition of the virial temperature is slightly different,

$$\frac{3}{2}kT_{\text{vir}} = \frac{1}{2}m_p\Omega_K^2R^2, \quad (16)$$

where Ω_K is the Keplerian velocity of the gas in the disk at radius R . In this work, we adopt $T_i = 0.9T_{\text{vir}}$ in all our calculations, which is almost equivalent to the value suggested by Liu et al. (2003).

It is still quite unclear on the outer radius of the accretion disk. One conventional estimate of the outer radius of the disk is based on the assumption that the disk is truncated where it becomes gravitational unstable (e.g., Collin & Zahn 2008). The outer radius of the disk is estimated with the Toomre parameter (Toomre 1964; Goldreich & Lynden-Bell 1965),

$$Q_{\text{Toomre}} = \frac{\Omega_K c_s}{2\pi G \rho H_d} = 1. \quad (17)$$

Given the values of the black hole mass M_{BH} , the spin parameter a , the viscosity parameter α , and the mass accretion rate \dot{M} , the disk structure can be derived by solving Equations (6)-(8) numerically. The structure of the corona is then available based on the derived disk structure by solving Equations (14)-(16).

3. Ray tracing method

The trajectory of the photons emitted from the inner region of the accretion disk-corona system is bent by the strong gravity of the black hole. The observed emergent spectrum of such an accretion disk-corona system surrounding a Kerr black hole can be calculated with the ray tracing method. We summarize the method briefly in this section.

In the Kerr spacetime, there are four constants for the motion of a photon (Carter 1968; Abramowicz & Fragile 2011), three of which can determine the trajectory of the photon, namely the energy at infinity,

$$E = -p_t, \quad (18)$$

the effective angular momentum,

$$L_z = p_\phi, \quad (19)$$

and the Carter constant,

$$Q = p_\theta^2 - a^2 E^2 \cos^2 \theta + L_z^2 \cot^2 \theta, \quad (20)$$

where p_μ is the four-momentum of the photon. Combining Equations (18)-(20) and the expressions of a photon's four-momentum in Carter (1968), we derive the following equations describing the trajectory of a photon in the Kerr spacetime:

$$\Sigma \frac{dr}{d\sigma} = \pm \sqrt{R(r)}, \quad (21)$$

$$\Sigma \frac{d\theta}{d\sigma} = \pm \sqrt{\Theta(\theta)}, \quad (22)$$

$$\Sigma \frac{d\phi}{d\sigma} = \frac{L_z}{\sin^2 \theta} + \frac{2arE - L_z a^2}{\Delta}, \quad (23)$$

$$\Sigma \frac{dt}{d\sigma} = -a(aE \sin^2 \theta - L_z) + \frac{(r^2 + a^2)[E(r^2 + a^2) - L_z a]}{\Delta}, \quad (24)$$

where

$$R(r) = [E(r^2 + a^2) - L_z a]^2 - \Delta[(L_z - aE)^2 + Q], \quad (25)$$

$$\Theta(\theta) = Q - \left(-a^2 E^2 + \frac{L_z^2}{\sin^2 \theta}\right) \cos^2 \theta. \quad (26)$$

Here σ is the affine parameter along the trajectory. The signs in the above equations must be the same as the signs of dr , $d\theta$ respectively, and they change at the turning point in r or θ , i.e., $R(r) = 0$ or $\Theta(\theta) = 0$. As the trajectory of a photon is independent of its energy E , Cunningham & Bardeen (1973) introduce two dimensionless parameters being conserved along the trajectory,

$$\lambda \equiv \frac{L_z}{E}, \quad q \equiv \frac{Q}{E^2} \quad (27)$$

and define another affine parameter $dP = E/\Sigma d\sigma$. The equations describing the trajectory of the photon can be re-written as

$$dr = \pm \sqrt{\tilde{R}(r)} dP, \quad (28)$$

$$d\theta = \pm \sqrt{\tilde{\Theta}(\theta)} dP, \quad (29)$$

$$d\phi = \left[\frac{\lambda}{\sin^2 \theta} + \frac{2ar - \lambda a^2}{\Delta} \right] dP, \quad (30)$$

$$dt = \left[\frac{(r^2 + a^2)^2}{\Delta} - a^2 \sin^2 \theta - \frac{2ar\lambda}{\Delta} \right] dP, \quad (31)$$

where $\tilde{R}(r) \equiv R(r)/E^2$, $\tilde{\Theta}(\theta) \equiv \Theta(\theta)/E^2$. Integrating the null geodesic equations of the photon along the path from the initial location $(r_{\text{em}}, \theta_{\text{em}}, \phi_{\text{em}})$ to the observer at infinity with position $(r_{\text{obs}}, \theta_{\text{obs}}, \phi_{\text{obs}})$, the trajectory can be determined by the following integral equations

$$\pm \int_{r_{\text{em}}}^{r_{\text{obs}}} \frac{dr}{\sqrt{\tilde{R}(r)}} = \pm \int_{\theta_{\text{em}}}^{\theta_{\text{obs}}} \frac{d\theta}{\sqrt{\tilde{\Theta}(\theta)}} = P, \quad (32)$$

and

$$\phi_{\text{obs}} - \phi_{\text{em}} = \pm \int_{P_{\text{em}}}^{P_{\text{obs}}} \left(\frac{\lambda}{\sin^2 \theta} + \frac{2ar - a^2 \lambda}{\Delta} \right) dP, \quad (33)$$

where $P_{\text{em}}, P_{\text{obs}}$ are functions of θ or r , corresponding to the upper limit value of the θ -integral taken as $\theta_{\text{em}}, \theta_{\text{obs}}$ respectively, and the signs in the above integrals must be the same as those of dr and $d\theta$ to guarantee the integral P is always positive and increasing along a photon's trajectory. In the calculations, we set $r_{\text{obs}} = \infty$, and $\phi_{\text{obs}} = 0$. The detailed explanation on the integrals can be found in some previous works (Chandrasekhar 1983; Cadez et al. 1998; Li et al. 2005).

The image of the accretion disk-corona observed at an angle θ_{obs} with respect to the axis of the black hole at infinity can be described by the two impact parameters,

$$\alpha = - \left(\frac{rp^{(\phi)}}{p^{(t)}} \right)_{r \rightarrow \infty} = - \frac{\lambda}{\sin \theta_{\text{obs}}}, \quad (34)$$

and

$$\beta = \left(\frac{rp^{(\theta)}}{p^{(t)}} \right)_{r \rightarrow \infty} = (q + a^2 \cos^2 \theta_{\text{obs}} - \lambda^2 \cot^2 \theta_{\text{obs}})^{1/2} = p_{\text{obs}}, \quad (35)$$

where α is the apparent displacement of the image perpendicular to the projected axis of the black hole, and β is the apparent parallel displacement. The vector $p^{(a)}$ is the four-momentum in the local nonrotating frame(LNRF). The observed image of the accretion

disk-corona can be calculated with the ray tracing method described above, provided that the local spectrum of the disk-corona is known. For a given point (α, β) in the image seen by the observer at $(\infty, \theta_{\text{obs}}, 0)$, the two constants of motion λ and q can be derived with Equations (34) and (35). Then the trajectory integral P , the radius r_{em} , and the azimuthal angle ϕ_{em} , can be calculated by using Equations (32) and (33).

4. Radiation transfer and emergent spectrum

In this work, the photons cannot move through the equatorial plane because of the optically thick accretion disk, and therefore we neglect such trajectories. For the photons passing through the corona, the optical depth for the scattering of photons in the corona in the curved space can be calculated with the ray tracing method. Along the trajectory of the photon in the corona, the differential optical depth is

$$d\tau = \sigma_T n_e dl, \quad (36)$$

where σ_T is the Thompson cross-section, n_e is the electrons number density in the corona at (R, z) , and

$$dl = e^\nu \Sigma dP = \pm \frac{e^\nu \Sigma}{\sqrt{\tilde{\Theta}(\theta)}} d\theta. \quad (37)$$

Integrating along the photon trajectory of the photon in the corona, we have

$$\tau = \pm \int_{\theta_{\text{em}}}^{\theta_{\text{obs}}} \frac{\sigma_T n_e e^\nu \Sigma}{\sqrt{\tilde{\Theta}(\theta)}} d\theta, \quad (38)$$

where $d\theta = \pm \sqrt{\tilde{\Theta}(\theta)} dP$.

As the accretion disk is geometrically thin, we approximate $\theta_{\text{em}} = \pi/2$ in calculating the emergent spectrum of the disk. The radiative flux from the accretion disk observed at infinity is given by

$$F(\nu_{\text{obs}}) = \int e^{-\tau} B_{\nu_{\text{obs}}} d\Omega = \int e^{-\tau} B_{\nu_{\text{obs}}} \frac{d\alpha d\beta}{D^2}, \quad (39)$$

where $B_{\nu_{\text{obs}}}$ is the intensity at observed frequency ν_{obs} , $d\Omega = d\alpha d\beta / D^2$ is the solid angle subtended by the image of the disk.

The gravitational redshift effect and Doppler redshift can be included by using the Lorentz invariant I/ν^3 (Rybicki & Lightman 1979), so the emergent spectrum can be calculated with

$$F(\nu_{\text{obs}}) = \int g^3 e^{-\tau} B_{\nu_e} \frac{d\alpha d\beta}{D^2} \quad (40)$$

where B_{ν_e} is the the intensity of the photons from the disk at emitting frequency ν_e . Integrating over the disk image, the emergent spectrum of the disk is available with

$$L_{\text{disk}}(\nu_{\text{obs}}) = 4\pi D^2 F(\nu_{\text{obs}}) = 4\pi \int g^3 e^{-\tau} B_{\nu_e} d\alpha d\beta. \quad (41)$$

The redshift factor is defined by (Cunningham & Bardeen 1973)

$$g \equiv \frac{\nu_{\text{obs}}}{\nu_e} = \frac{p_\mu u^\mu|_{\text{obs}}}{p_\mu u^\mu|_{\text{em}}}, \quad (42)$$

where p_μ is the four-momentum of the photon (Carter 1968),

$$p_\mu = (p_t, p_r, p_\theta, p_\phi) = (-1, \pm \frac{\sqrt{\tilde{R}(r)}}{\Delta}, \pm \sqrt{\tilde{\Theta}(\theta)}, \lambda) E. \quad (43)$$

The four-velocity of the fluid in the locally non-rotating frame (LNRF) u_{obs}^μ and the local rest frame (LRF) u_{em}^μ are given by

$$u_{\text{obs}}^\mu = (1, 0, 0, 0), \quad (44)$$

and

$$u_{\text{em}}^\mu = (\gamma_r \gamma_\phi e^{-\nu}, \gamma_r \beta_r e^{-\mu_1}, 0, \gamma_r \gamma_\phi (\omega e^{-\nu} + \beta_\phi e^{-\psi})), \quad (45)$$

respectively (Yuan et al. 2009).

The corona is assumed to rotate with the disk at Keplerian velocity. The calculations of the emergent spectrum of the corona is slightly different from that of the accretion disk, because the redshift factor g and the trajectory of a photon depends on the location of the photon emitted ($r_{\text{em}}, \phi_{\text{em}}, z_{\text{em}}$) in the corona. To calculate the redshift factor g and the trajectory of such a photon, we numerically solve Equations (32) and (33) to derive the impact parameters α and β . We divide the corona into small volumes with $dh d\epsilon$ where $d\epsilon$ is element area and dh is the thickness of a layer, and the emergent spectrum of each volume is available by calculating the radiation transfer with the ray tracing method, if the emissivity of the corona is available. For simplicity, we assume the radiation of the corona to be isotropic and the emissivity is homogeneous in the vertical direction of the corona.

The synchrotron and bremsstrahlung emissivities are taken from Narayan & Yi (1995). The spectrum of synchrotron and bremsstrahlung emission from the corona is available by summing up the contribution from these small volumes,

$$L_{\text{syn,brem}} = 4\pi \int g_h^3 e^{-\tau_h} (\varepsilon_{\nu_e}^{\text{syn}} + \varepsilon_{\nu_e}^{\text{brem}}) d\alpha d\beta, \quad (46)$$

where the effects of the absorption and the scattering in the corona are considered as described at the beginning of this section.

In the calculations of the Comptonization in the corona, we assume the corona to be a parallel plane (see Cao 2009, for the details). The mean probability of the soft photons injected from the cold disk experiencing first-order scattering in the corona is

$$P_1 = 2 \int_0^1 (1 - e^{-\tau_0/\cos\theta}) \cos\theta d\cos\theta, \quad (47)$$

where the constant specific intensity of the soft photons from the disk is assumed, θ is the angle of the motion of the soft photons with respect to the vertical direction of the disk, and $\tau_0 = \sigma_T n_e H_{\text{cor}}$ is the optical depth of the corona for electron scattering in the vertical direction. We can calculate the first-order Comptonized spectra of the corona $F_{\nu,1}^{\text{Comp}}$ using the method suggested by Coppi & Blandford (1990) with the probability given by Equation (47), if the density and the temperature of electrons in the corona, and the incident spectrum of the cold disk are known. As we have assumed the scattered photons to be isotropic, the emissivity of the first-order Compton scattered photons in the layer with the height between h and $h + dh$ can be approximated as $\epsilon_{\nu,1}^{\text{Comp}}(R_d) = F_{\nu,1}^{\text{Comp}} dh/H_{\text{cor}}$. The first-order Compton scattered photons will pass through the corona before arriving the observer. Using the above described ray tracing approach, we can calculate the emergent first-order Comptonized spectrum of the corona.

The mean probability for these first-order scattered photons experiencing the second-order scattering can be estimated as

$$P_2 = \frac{1}{2} \int_0^1 d\xi \int_0^1 [1 - e^{-\xi\tau_0/\cos\theta} + 1 - e^{-(1-\xi)\tau_0/\cos\theta}] d\cos\theta, \quad (48)$$

where $\xi = z/H_{\text{cor}}$, and the first-order scattered photons are assumed to be radiated isotropically. The two terms in the integration are for downward-moving and upward-moving photons emitted at height z , respectively. The probability of the scattered photons experiencing next higher order scattering approximates to P_2 , so we simply adopt $P_n = P_2$ for $n > 2$. Thus, the n th-order Comptonized spectra $F_{\nu,n}^{\text{Comp}}$ and emissivity $\epsilon_{\nu,n}^{\text{Comp}}$ can be derived with the same method for calculating the first-order Comptonization, in which the $(n-1)$ th-order Comptonized spectra are used instead of the incident spectrum from the cold disk used for the calculation of the first-order Comptonization. In the same way, the emergent spectra of high order Comptonized spectra are derived, and the total Comptonized spectrum of the corona is available by summing up the contribution from the whole corona,

$$L_{\text{Comp}} = 4\pi \int g_h^3 (\epsilon_{\nu,1}^{\text{Comp}} + \epsilon_{\nu,2}^{\text{Comp}} + \dots + \epsilon_{\nu,n}^{\text{Comp}}) d\alpha d\beta. \quad (49)$$

5. Results

As described in Section 2, we can calculate the structure of an accretion disk with corona surrounding a rotating Kerr black hole, if the black hole mass M_{bh} , the spin parameter a , and the dimensionless accretion rate \dot{m} are specified. Based on the derived structure of the accretion disk-corona system, the emergent spectrum observed at infinity with an inclination angle θ_{obs} is calculated with the ray tracing method described in Sections 3 and 4, in which all the general relativistic effects are considered. The black hole mass $M_{\text{bh}} = 10^8 M_{\odot}$ is adopted in most of our calculations for AGNs. The dimensionless mass accretion rate is defined as $\dot{m} = \dot{M}/\dot{M}_{\text{Edd}}$ ($\dot{M}_{\text{Edd}} = L_{\text{Edd}}/0.1c^2$) independent of black hole spin.

We plot the ratios of the power dissipated in the corona to the total released gravitational power $L_{\text{cor}}/L_{\text{bol}}$ as functions of the accretion rate \dot{m} with different values of the black hole spin parameter a in Figure 1. It is found that the dependence of the ratio $L_{\text{cor}}/L_{\text{bol}}$ with \dot{m} is quite different for the cases with different magnetic stress tensors, which are qualitatively consistent with those obtained in Cao (2009) for the Newtonian accretion disk corona model. We find that the ratio $L_{\text{cor}}/L_{\text{bol}}$ decreases with increasing spin parameter a with either $\tau_{\text{r}\varphi} = \alpha P_{\text{gas}}$ or $\tau_{\text{r}\varphi} = \alpha \sqrt{P_{\text{gas}} P_{\text{tot}}}$ if all other parameters are fixed, which means that the efficiency of the energy transportation from the disk to the corona is low for a rapidly spinning black hole independent of the detailed magnetic stress tensor adopted. However the model with $\tau_{\text{r}\varphi} = \alpha P_{\text{tot}}$ appears to show the opposite trend that $L_{\text{cor}}/L_{\text{bol}}$ reaches large values for a rapidly spinning black hole.

In Figure 2, we plot the interior temperatures of the accretion disks as functions of radius R with different values of the accretion rate \dot{m} and black hole spin parameter a , and the stress $\tau_{\text{r}\varphi} = \alpha \sqrt{P_{\text{gas}} P_{\text{tot}}}$ is adopted in the calculations. It is not surprising that the temperature of the disk increases with the mass accretion rate \dot{m} . For a rapidly spinning black hole, the inner edge of the disk extends to the region close to the black hole, and the temperature of the gas in the inner edge of the disk is significantly higher than that for a slowly spinning (or non-spinning) black hole.

The structures of the corona calculated with $\tau_{\text{r}\varphi} = \alpha \sqrt{P_{\text{gas}} P_{\text{tot}}}$, i.e., the temperatures of the ions and electrons, and the electron scattering optical depth of the corona in the vertical direction, are plotted in Figure 3. The electron temperature decreases with increasing mass accretion rate \dot{m} and the black hole spin parameter a . The optical depth for electron scattering is in the range of $\sim 0.1 - 0.3$ for different values of \dot{m} and a adopted.

The emergent spectra of the accretion disk-corona systems with $\tau_{\text{r}\varphi} = \alpha \sqrt{P_{\text{gas}} P_{\text{tot}}}$ observed at infinity with different disk model parameters and viewing angles are plotted in Figure 4. In each panel, one of these parameters is fixed at a certain value and the other

ones are taken as free parameters in the calculations of the emergent spectra. The corona is optically thin and geometrically thick, and therefore its radiation is almost isotropic. The radiation of the disk is dominantly in the optical/UV bands, the emergent spectrum of which depends on the viewing angle sensitively due to its slab-like geometry. The photon spectral indices, and the ratios of the bolometric luminosity to the X-ray luminosity in 2 – 10 keV as functions of the accretion rate \dot{m} for different values of a and θ_{obs} are plotted in Figure 5. The hard X-ray spectral index Γ increases with the accretion rate \dot{m} and black hole spin a , while it is insensitive with inclination θ_{obs} . The ratio of the bolometric luminosity to the X-ray luminosity increases with mass accretion rate, which is higher for a rapidly spinning black hole.

The calculated emergent spectrum is usually insensitive to the outer radius of the accretion disk, except the spectral shape in the infrared/optical wavebands. The outer radius of the accretion disk can be estimated by assuming the disk to be truncated where the self-gravity of the disk dominates over the central gravity of the black hole. The outer radii of the accretion disks with different accretion rates \dot{m} and black hole masses M_{bh} are plotted in Figure 6. The results show that the accretion disk surround a less massive black hole extends to a larger radius. The spectral shape of the accretion disk in the infrared/optical wavebands also varies with the outer radius of the disk R_{out} . We plot the emergent spectra of the disk-corona systems with $\tau_{\text{r}\phi} = \alpha\sqrt{P_{\text{gas}}P_{\text{tot}}}$ in the near-infrared/optical wavebands with different values of the accretion rate \dot{m} and black hole spin parameter a in Figure 7. We find that the spectral shapes of the accretion disk-corona systems deviate significantly from $f_{\nu} \propto \nu^{1/3}$, which is predicted by the standard accretion disk model (Shakura & Sunyaev 1973; Koratkar & Blaes 1999; Hubeny et al. 2000). Davis et al. (2007) measured UV spectral slopes (s , where $f_{\nu} \propto \nu^s$) for several thousand quasars from the Sloan Digital Sky Survey (SDSS), and the distributions of the slope s span a wide range rather than $s = 1/3$ predicted by the standard accretion model.

6. Discussion

In this work, we calculate the structure of an accretion disk with corona around a Kerr black hole, and the emergent spectrum of the system is derived with the ray tracing approach, in which the general relativistic effects have been considered. The ions and electrons in the corona are assumed to be heated by magnetic power with the reconnection of the buoyant magnetic fields transported from the disk (Di Matteo 1998). The strength of the magnetic fields can be estimated from gas/radiation pressure of the disk with assumed magnetic stress tensor. We examine the relations of the ratio $L_{\text{cor}}/L_{\text{bol}}$ with the mass accretion rate \dot{m} in

the models with different magnetic stress tensors (see Figure 1). In order to understand the results, we analyze the situation based on the standard thin disk model. The gravitational power dissipated in unit surface area of the accretion disk is given by (Shakura & Sunyaev 1973)

$$Q_{\text{dissi}}^+ = \frac{1}{2} W_{r\varphi} R \frac{d\Omega_k}{dr} = \frac{3}{2} \tau_{r\varphi} H_d \Omega_k = \frac{3}{2} \tau_{r\varphi} c_s = \frac{3}{2} \tau_{r\varphi} \left(\frac{p_{\text{tot}} + p_m}{\rho} \right)^{1/2} \quad (50)$$

where $W_{r\varphi} = \int_{-H_d}^{H_d} \tau_{r\varphi} dh$, $p_{\text{tot}} = p_{\text{gas}} + p_{\text{rad}}$. The power dissipated in the corona is

$$Q_{\text{cor}}^+ = p_m v_p = b v_A p_m = \frac{b p_m B}{(4\pi\rho)^{1/2}} = b p_m \left(\frac{2p_m}{\rho} \right)^{1/2} \quad (51)$$

Combining Equations (50) and (51), we find that the ratio $L_{\text{cor}}/L_{\text{bol}} \propto p_m/(p_m + p_{\text{tot}})$. If the stress tensor $\tau_{r\varphi} = p_m = \alpha p_{\text{tot}}$ is adopted, the ratio $L_{\text{cor}}/L_{\text{bol}}$ remains constant independent of accretion rate \dot{m} . For the cases of $\tau_{r\varphi} = p_m = \alpha p_{\text{gas}}$, or $\tau_{r\varphi} = \alpha \sqrt{p_{\text{gas}} p_{\text{tot}}}$, the ratio $L_{\text{cor}}/L_{\text{bol}} \propto T_d^{-3}$ or $T_d^{-3/2}$ respectively, as $p_{\text{gas}} \sim T_d$, $p_{\text{rad}} \sim T_d^4$ and the radiation pressure is dominant in the inner regions of the accretion disk. As the disk temperature increases with mass accretion rate \dot{m} , the ratio $L_{\text{cor}}/L_{\text{bol}}$ therefore decreases with increasing \dot{m} . The results obtained in this work for spinning black holes are qualitatively consistent with those derived in Cao (2009).

As the value of black hole spin parameter a increases, the disk extends close to the black hole, and more gravitational power is released in the inner region of the accretion disk. The temperature of the inner disk region T_d increases with the spin parameter a , which increases the energy density of the soft photons emitted from the disk. This leads to the corona cooling efficiently, because the cooling of the corona is dominated by the Compton scattering of the soft photons from the disk. The electron temperature of the corona in the inner region of the disk is therefore lower for rapidly spinning black holes (see Figure 3).

The resulted spectra of the disk-corona systems with magnetic stress tensor $\tau_{r\varphi} = \alpha \sqrt{p_{\text{gas}} p_{\text{tot}}}$ show that both the hard X-ray spectral index and the hard X-ray bolometric correction factor $L_{\text{bol}}/L_{X,2-10\text{keV}}$ increase with the Eddington ratio, which are qualitatively consistent with the observations of AGNs (Wang et al. 2004; Shemmer et al. 2006; Vasudevan & Fabian 2007), and X-ray binaries (Wu & Gu 2008). The observed ratio of $L_{\text{opt}}/L_{\text{bol}}$ may provide additional information of the disk-corona systems (Davis & Laor 2011). The stress tensor $\tau_{r\varphi} = \alpha \sqrt{p_{\text{gas}} p_{\text{tot}}}$ was initially suggested by Taam & Lin (1984) based on the idea that the viscosity is proportional to the gas pressure, but the size of turbulence should be limited by the disk scale height determined by the total pressure. This is also supported by the analysis on the local dynamical instabilities in magnetized, radiation-

pressure-supported accretion disks (Blaes & Socrates 2001; Merloni & Fabian 2002). However, recent radiative MHD simulations seem to prefer the stress tensor $\tau_{r\varphi} = \alpha p_{\text{tot}}$ (Hirose et al. 2009). Our model calculations can be carried out when the form of magnetic stress tensor is specified. For simplicity, in most cases of this work, we calculate the structure and emergent spectra of accretion disk-corona systems using the magnetic stress tensor $\tau_{r\varphi} = \alpha\sqrt{p_{\text{gas}}p_{\text{tot}}}$.

The radiation from the corona is almost isotropic due to its optically thin and geometrically thick structure, while the radiation from the disk is anisotropic. It is therefore found that the hard X-ray spectral index Γ is insensitive with the viewing angle θ_{obs} . The X-ray spectra are mainly dominated by the inverse Compton scattering, which mainly depends on the temperature of the electrons. Therefore the trend of the photon spectral indices Γ and the X-ray correction factors $L_{\text{bol}}/L_{\text{X},2-10\text{keV}}$ can be explained by the decrease of the temperature of the electrons with increasing mass accretion rate \dot{m} , or the black hole spin parameter a (see Figure 5, and also Figure 3). The photon index Γ of the hard X-ray spectrum becomes large when the black hole is rapidly spinning if all other parameters are fixed, which is due to the temperature of the electrons decreases with increasing value of a . The correction factor $L_{\text{bol}}/L_{\text{X},2-10\text{keV}}$ derived by the model calculations with $\tau_{r\varphi} = \alpha\sqrt{p_{\text{gas}}p_{\text{tot}}}$ are significantly larger than the observed values when $\dot{m} \sim 0.1$ (e.g., Wang et al. 2004; Vasudevan & Fabian 2007). One possibility is that an advection dominated accretion flow (ADAF) is present in the inner region of the disk (Narayan & Yi 1994, 1995). The inner ADAF is X-ray luminous, which leads to a low value of $L_{\text{bol}}/L_{\text{X},2-10\text{keV}}$ (Quataert et al. 1999). This is also consistent with the fact that the X-ray spectra of the AGNs are hard when accreting at low rates (see Wang et al. 2004; Cao 2009, for the detailed discussion). An alternative resolution is the model with magnetic stress tensor $\tau_{r\varphi} = \alpha p_{\text{tot}}$, however, it always predicts a constant $L_{\text{bol}}/L_{\text{X},2-10\text{keV}}$ independent of mass accretion rate \dot{m} . This needs further investigations in the future.

In Figure 7, the spectral shapes of the disk-corona model with different values of accretion rates \dot{m} and black hole spin parameter a in the near-infrared/optical bands are plotted, which is dominantly contributed by the blackbody radiation from the disk. The spectral shapes are significantly different from $f_{\nu} \propto \nu^{1/3}$, as expected in standard thin disk model. This is mainly caused by the R -dependent temperature distributions in the disks surrounding massive black holes and the outer radii of the disks being different from those in standard thin disk model. In the standard thin disk model, the spectral shape $f_{\nu} \propto \nu^{1/3}$ in the near-infrared/optical wavebands is derived by assuming the temperature of the accretion disk $T_{\text{d}} \sim R^{-3/4}$ and the disk to extend to infinity. However, the temperature profiles of relativistic accretion disks deviate significantly from $T_{\text{d}} \sim R^{-3/4}$ in the inner region of the disk ($R < 100R_{\text{S}}$) (see Figure 2). The contribution to the spectra in IR/optical bands from the blackbody radiation of the outer region of the disks can also be quite important. The

outer radius of the disk is a function of black hole mass M_{bh} and accretion rate \dot{m} (see Figure 6). The observational slope of the infrared continua can be used to constrain the accretion disk model (see Kishimoto et al. 2008). It is not suitable to compare the observed spectra only with, $f_\nu \propto \nu^{1/3}$, as predicted by the standard accretion disk model. In this work, the local radiation from the disk is approximated as blackbody emission. A better approximation is to include a spectral hardening factor in calculating the local spectrum of the disk (e.g., Shimura & Takahara 1995; Hubeny et al. 2000; Davis et al. 2007), with which the energy peak of the calculated disk spectrum will shift to a slightly higher frequency, while the spectral shape changes little. This would be important for detailed fitting the observed SED of AGNs, which is beyond the scope of this paper.

It is assumed that zero torque at the inner edge of the disk (Shakura & Sunyaev 1973), which was doubted in some previous works (Agol & Krolik 2000; Hawley & Krolik 2001). The general relativistic magnetohydrodynamic (GRMHD) simulations provide an effective tool to explore the torque in the plunging region (Shafee et al. 2008; Kulkarni et al. 2011). In the accretion disk with the thickness $h/r \sim 0.05 - 0.1$ the magnetic torque at the radius of the innermost stable circular orbit (ISCO) is only $\sim 2\%$ of the inward flux of angular momentum at this radius, which indicates that the zero torque is really a good approximation for geometrically thin disks (Shafee et al. 2008). Gong et al. (2012) investigated the accretion disk-corona model similar to that developed by Cao (2009), in which a non-zero torque at the inner edge of the disk is assumed. As the detailed accretion physics in the plunging region is complicated and still quite unclear, we adopt the assumption of no torque in the inner edge of the accretion disk in all our calculations. The calculations in this work were carried out for massive black holes, which will be compared with the observed spectra of AGNs in our future work. The model calculations can also be applicable to X-ray binaries.

Acknowledgements

This work is supported by the National Basic Research Program of China (grant 2009CB824800, 2012CB821800), the NSFC (grants grants 11173043, 11121062, 11233006, 11073020, and 11133005), the CAS/SAFEA International Partnership Program for Creative Research Teams (KJCX2-YW-T23), and the Fundamental Research Funds for the Central Universities (WK2030220004).

REFERENCES

- Abramowicz, M. A., & Fragile, P. C. 2011, arXiv:1104.5499
- Agol, E., & Krolik, J. H. 2000, *ApJ*, 528, 161
- Balbus, S. A., & Hawley, J. F. 1991, *ApJ*, 376, 214
- Bisnovatyi-Kogan, G. S., & Lovelace, R. V. E. 1997, *ApJ*, 486, L43
- Bisnovatyi-Kogan, G. S., & Lovelace, R. V. E. 2000, *ApJ*, 529, 978
- Blaes, O., & Socrates, A. 2001, *ApJ*, 553, 987
- Cadez, A., Fanton, C., Calvani, M., & Marziani, P. 1998, 19th Texas Symposium on Relativistic Astrophysics and Cosmology,
- Cao, X. 2009, *MNRAS*, 394, 207
- Carter, B. 1968, *Physical Review*, 174, 1559
- Chandrasekhar, S. 1983, Research supported by NSF. Oxford/New York, Clarendon Press/Oxford University Press (International Series of Monographs on Physics. Volume 69), 1983, 663 p.,
- Collin, S., & Zahn, J.-P. 2008, *A&A*, 477, 419
- Coppi, P. S., & Blandford, R. D. 1990, *MNRAS*, 245, 453
- Cunningham, C. T., & Bardeen, J. M. 1973, *ApJ*, 183, 237
- Czerny, B., Hryniewicz, K., Nikolajuk, M., & Sądowski, A. 2011, *MNRAS*, 415, 2942
- Davis, S. W., & Laor, A. 2011, *ApJ*, 728, 98
- Davis, S. W., Woo, J.-H., & Blaes, O. M. 2007, *ApJ*, 668, 682
- Di Matteo, T. 1998, *MNRAS*, 299, L15
- Di Matteo, T., Celotti, A., & Fabian, A. C. 1999, *MNRAS*, 304, 809
- Fuerst, S. V., & Wu, K. 2004, *A&A*, 424, 733
- Galeev, A. A., Rosner, R., & Vaiana, G. S. 1979, *ApJ*, 229, 318
- Goldreich, P., & Lynden-Bell, D. 1965, *MNRAS*, 130, 97

- Gong, X.-L., Li, L.-X., & Ma, R.-Y. 2012, MNRAS, 420, 1415
- Gou, L., McClintock, J. E., Reid, M. J., et al. 2011, ApJ, 742, 85
- Haardt, F., & Maraschi, L. 1991, ApJ, 380, L51
- Hawley, J. F., & Krolik, J. H. 2001, ApJ, 548, 348
- Hirose, S., Blaes, O., & Krolik, J. H. 2009, ApJ, 704, 781 2012
- Hu, R., & Zhang, S.-N. 2012, arXiv:1206.2569
- Hubeny, I., Agol, E., Blaes, O., & Krolik, J. H. 2000, ApJ, 533, 710
- Kawaguchi, T., Shimura, T., & Mineshige, S. 2001, ApJ, 546, 966
- Kishimoto, M., Antonucci, R., Blaes, O., et al. 2008, Nature, 454, 492
- Koratkar, A., & Blaes, O. 1999, PASP, 111, 1
- Kulkarni, A. K., Penna, R. F., Shcherbakov, R. V., et al. 2011, MNRAS, 414, 1183
- Laor, A., & Netzer, H. 1989, MNRAS, 238, 897
- Laor, A. 1990, MNRAS, 246, 369
- Laor, A. 1991, ApJ, 376, 90
- Li, G.-X., Yuan, Y.-F., & Cao, X. 2010, ApJ, 715, 623
- Li, L.-X., Zimmerman, E. R., Narayan, R., & McClintock, J. E. 2005, ApJS, 157, 335
- Li, Y.-R., Yuan, Y.-F., Wang, J.-M., Wang, J.-C., & Zhang, S. 2009, ApJ, 699, 513
- Liu, B. F., Mineshige, S., & Shibata, K. 2002, ApJ, 572, L173
- Liu, B. F., Mineshige, S., & Ohsuga, K. 2003, ApJ, 587, 571
- Malkan, M. A., & Sargent, W. L. W. 1982, ApJ, 254, 22
- McClintock, J. E., Narayan, R., Davis, S. W., et al. 2011, Classical and Quantum Gravity, 28, 114009
- McClintock, J. E., Shafee, R., Narayan, R., et al. 2006, ApJ, 652, 518
- Merloni, A., & Fabian, A. C. 2001, MNRAS, 328, 958

- Merloni, A., & Fabian, A. C. 2002, MNRAS, 332, 165
- Miller, J. M. 2007, ARA&A, 45, 441
- Narayan, R., & Yi, I. 1994, ApJ, 428, L13
- Narayan, R., & Yi, I. 1995, ApJ, 452, 710
- Novikov, I. D., & Thorne, K. S. 1973, Black Holes (Les Astres Occlus), 343
- Page, D. N., & Thorne, K. S. 1974, ApJ, 191, 499
- Quataert, E., Di Matteo, T., Narayan, R., & Ho, L. C. 1999, ApJ, 525, L89
- Rauch, K. P., & Blandford, R. D. 1994, ApJ, 421, 46
- Riffert, H., & Herold, H. 1995, ApJ, 450, 508
- Rybicki, G. B., & Lightman, A. P. 1979, New York, Wiley-Interscience, 1979. 393 p.,
- Sakimoto, P. J., & Coroniti, F. V. 1981, ApJ, 247, 19
- Schnittman, J. D., & Krolik, J. H. 2010, ApJ, 712, 908
- Shafee, R., McKinney, J. C., Narayan, R., et al. 2008, ApJ, 687, L25
- Shakura, N. I., & Sunyaev, R. A. 1973, A&A, 24, 337
- Shemmer, O., Brandt, W. N., Netzer, H., Maiolino, R., & Kaspi, S. 2006, ApJ, 646, L29
- Shields, G. A. 1978, Nature, 273, 519
- Shimura, T., & Takahara, F. 1995, ApJ, 445, 780
- Steiner, J. F., McClintock, J. E., Remillard, R. A., Narayan, R., & Gou, L. 2009, ApJ, 701, L83
- Stella, L., & Rosner, R. 1984, ApJ, 277, 312
- Stepney, S., & Guilbert, P. W. 1983, MNRAS, 204, 1269
- Sun, W.-H., & Malkan, M. A. 1989, ApJ, 346, 68
- Svensson, R., & Zdziarski, A. A. 1994, ApJ, 436, 599
- Taam, R. E., & Lin, D. N. C. 1984, ApJ, 287, 761

- Toomre, A. 1964, *ApJ*, 139, 1217
- Vasudevan, R. V., & Fabian, A. C. 2007, *MNRAS*, 381, 1235
- Wang, J.-M., Watarai, K.-Y., & Mineshige, S. 2004, *ApJ*, 607, L107
- Wu, Q., & Gu, M. 2008, *ApJ*, 682, 212
- Yuan, W., Liu, B. F., Zhou, H., & Wang, T. G. 2010, *ApJ*, 723, 508
- Yuan, Y.-F., Cao, X., Huang, L., & Shen, Z.-Q. 2009, *ApJ*, 699, 722
- Zdziarski, A. A., Lubinski, P., & Smith, D. A. 1999, *MNRAS*, 303, L11
- Zhang, J. L., Xiang, S. P., & Lu, J. F. 1985, *Ap&SS*, 113, 181
- Zhang, S. N., Cui, W., & Chen, W. 1997, *ApJ*, 482, L155

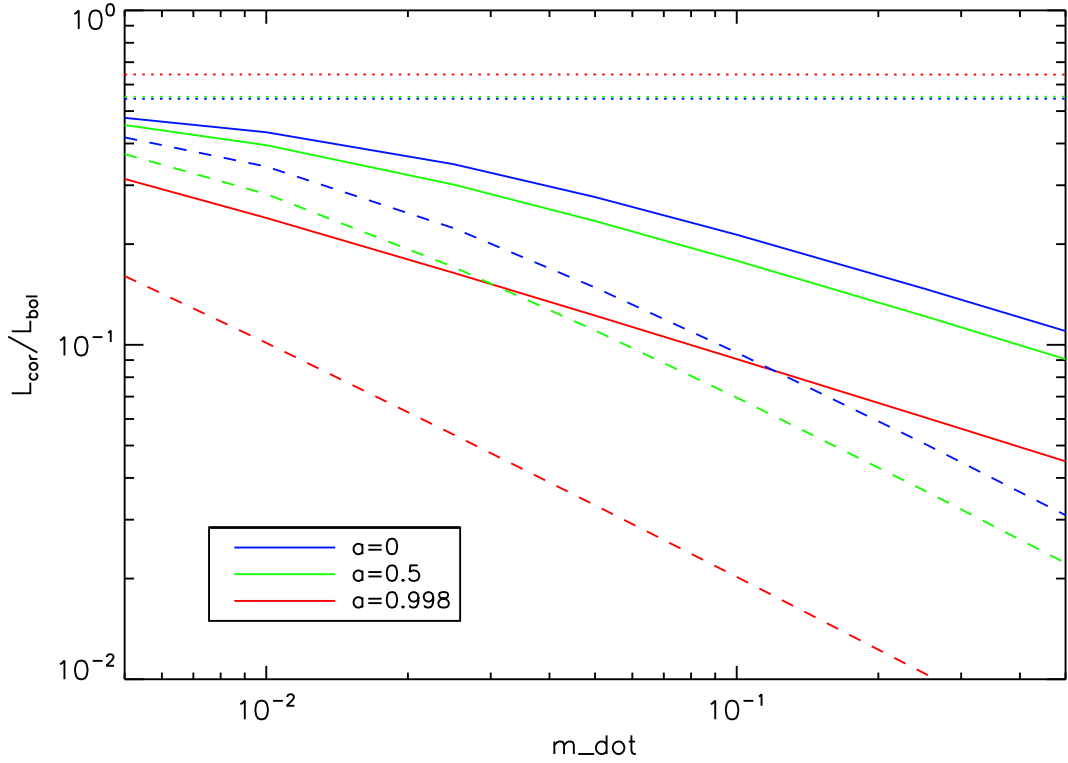


Fig. 1.— The ratios $L_{\text{cor}}/L_{\text{bol}}$ as functions of accretion rate \dot{m} with different magnetic stress tensors. The color lines represent different values of black hole spin parameter, i.e., $a = 0$ (blue), 0.5 (green), and 0.998 (red). The different type lines correspond to different magnetic stress tensors, i.e., $\tau_{r\varphi} = \alpha p_{\text{tot}}$ (dotted lines), $\tau_{r\varphi} = \alpha \sqrt{p_{\text{gas}} p_{\text{tot}}}$ (solid lines), and $\tau_{r\varphi} = \alpha p_{\text{gas}}$ (dashed lines).

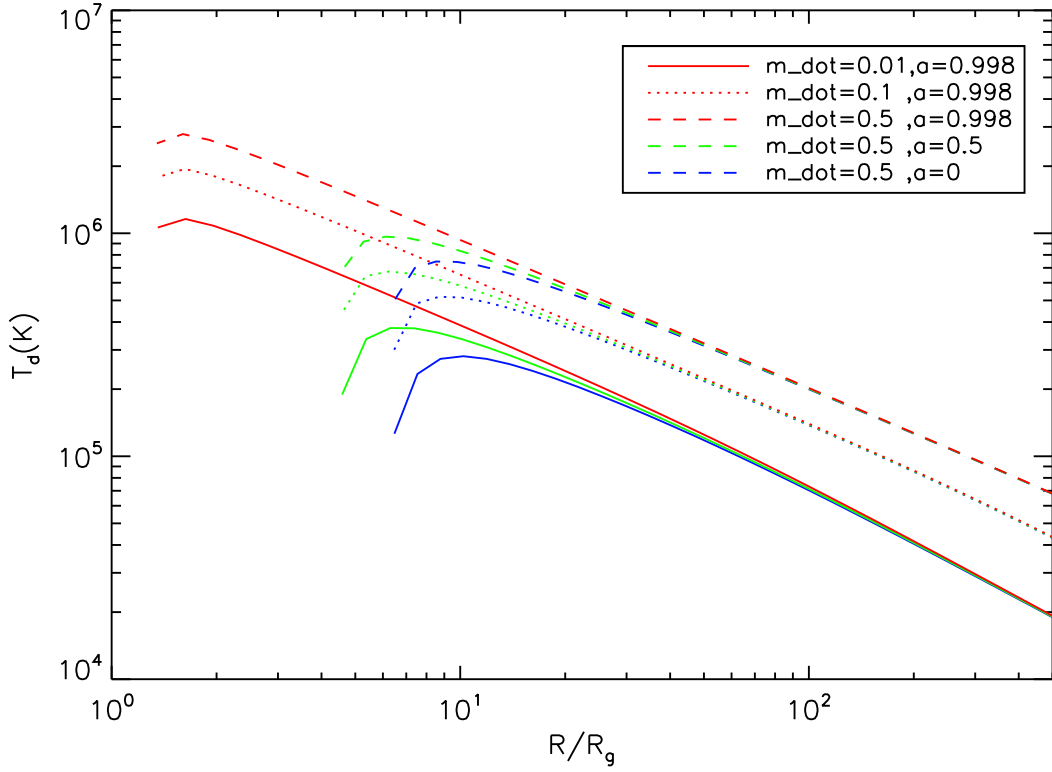


Fig. 2.— The temperatures in the mid-plane of the accretion disks as functions of radius R in units of $R_g = GM_{\text{bh}}/c^2$ with different values of accretion rate \dot{m} and black hole spin parameter a . The colored lines represent the model results with different values of black hole spin parameter, i.e., $a = 0$ (blue), 0.5 (green), and 0.998 (red). The solid lines represent the results calculated with $\dot{m} = 0.01$, while the dotted and dash lines are for $\dot{m} = 0.1$ and 0.5 , respectively. The stress $\tau_{r\varphi} = \alpha \sqrt{P_{\text{gas}} P_{\text{tot}}}$ is adopted.

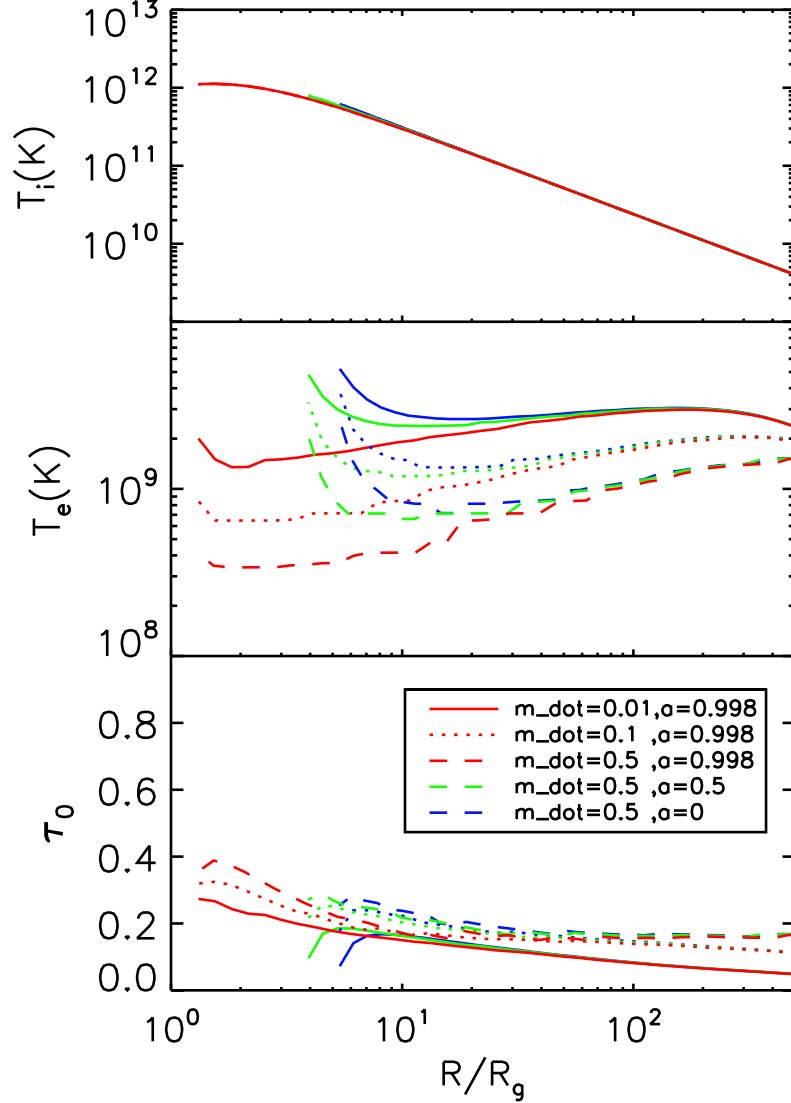


Fig. 3.— The upper panel: the temperatures of the ions in the coronae as functions of radius R with $\tau_{r\varphi} = \alpha \sqrt{P_{\text{gas}} P_{\text{tot}}}$. The middle panel: the temperatures of the hot electrons in the coronae. The lower panel: the optical depth for the Compton scattering of the electrons in the vertical direction of the coronae. The colored lines represent different values of black hole spin parameter, i.e., $a = 0.998$ (red), 0.5 (green), and 0 (blue). The solid lines represent the results calculated with $\dot{m} = 0.01$, while the dotted and dash lines are for $\dot{m} = 0.1$ and 0.5 , respectively.

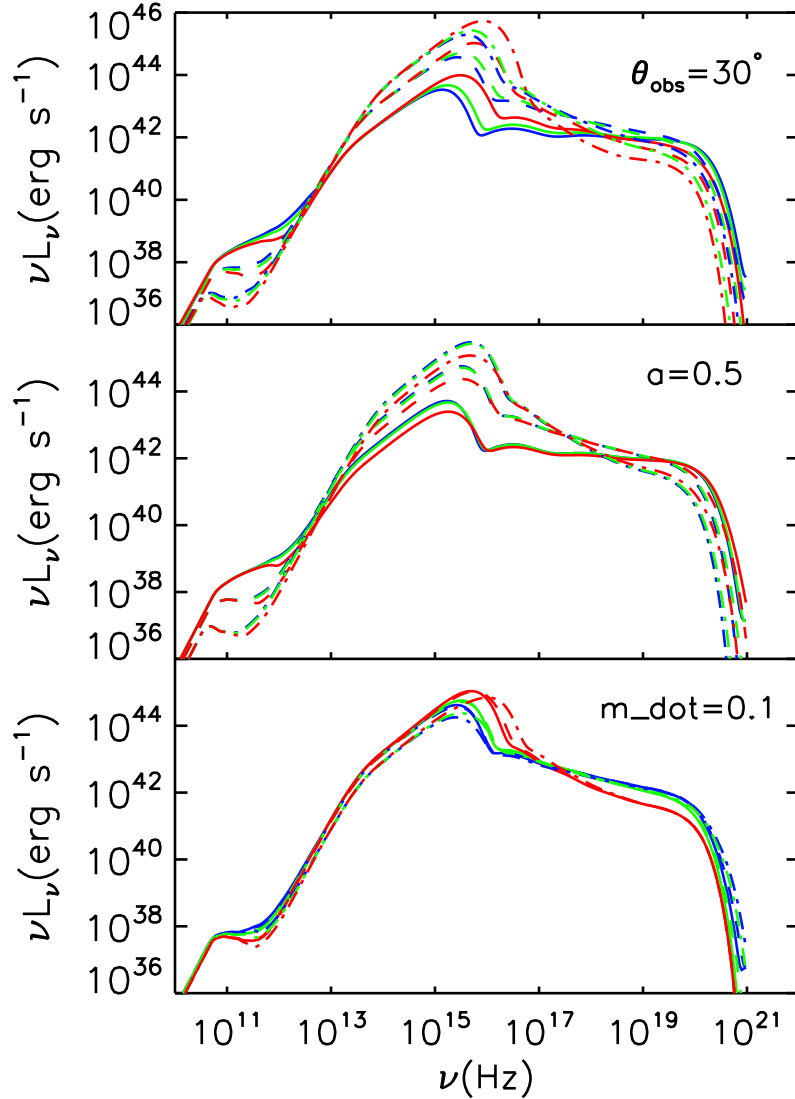


Fig. 4.— The spectra of the disk-corona systems with different values of \dot{m} , a , and θ_{obs} . The upper panel: the emergent spectra of the disk-corona systems surrounding spinning black holes observed at an angle $\theta_{\text{obs}} = 30^\circ$ with respect to the disk axis (red: $a = 0.998$, green: $a = 0.5$, and blue: $a = 0$). The different type lines represent the spectra calculated with different values of accretion rate, i.e., $\dot{m} = 0.5$ (dash-dotted), 0.05 (dashed), and 0.01 (solid). The middle panel: the spectra of the disk-corona systems surrounding black holes spinning at $a = 0.5$. The different colored lines represent the emergent spectra observed at different inclination angles, i.e., $\theta_{\text{obs}} = 60^\circ$ (red), 30° (green), and 10° (blue). The different type lines represent the different values of accretion rate, i.e., $\dot{m} = 0.5$ (dash-dotted), 0.05 (dashed), and 0.01 (solid). The bottom panel: the spectra of the disk-corona systems calculated with a given accretion rate, $\dot{m} = 0.1$. The different colored lines represent the spectra with different values of black hole spin parameter, i.e., $a = 0.998$ (red), 0.5 (green), and 0 (blue). The spectra observed at different angles are plotted with different type lines, i.e., $\theta_{\text{obs}} = 60^\circ$ (dash-dotted), 30° (dashed), and 10° (solid). The stress $\tau_{r\varphi} = \alpha \sqrt{P_{\text{gas}} P_{\text{tot}}}$ is adopted in the calculations.

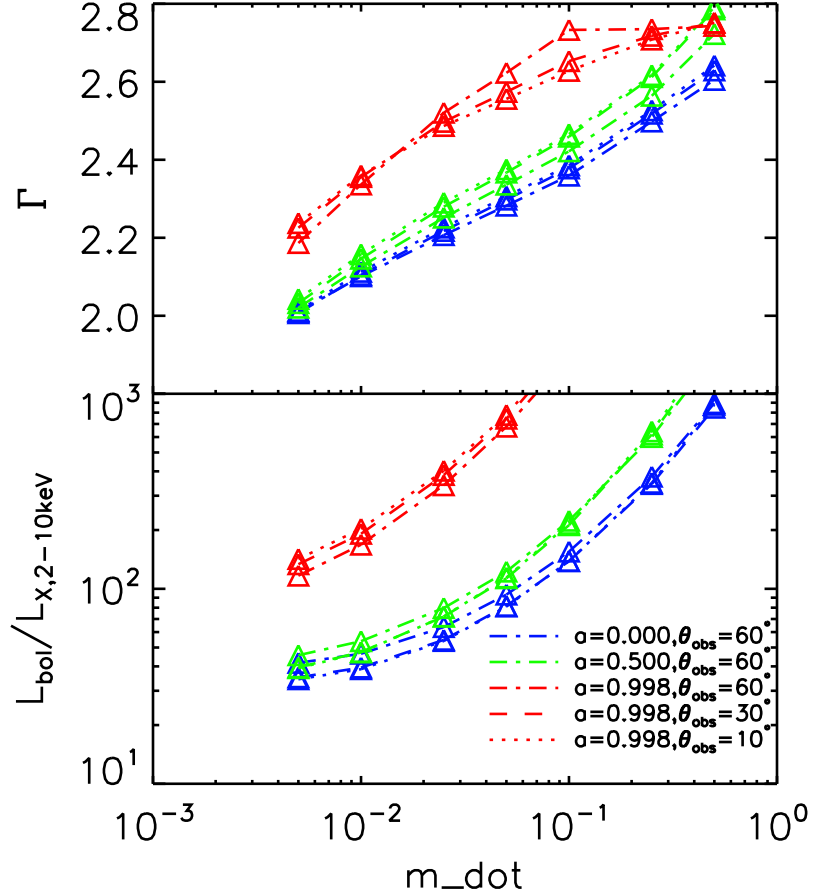


Fig. 5.— The upper panel: the photon spectral indices as functions of accretion rate \dot{m} for different values of black spin parameter a and viewing angle θ_{obs} with $\tau_{\text{r}\varphi} = \alpha \sqrt{P_{\text{gas}} P_{\text{tot}}}$. The lower panel: the X-ray bolometric correction factors $L_{\text{bol}}/L_{X,2-10\text{keV}}$ as functions of accretion rate \dot{m} for different model parameters. The colored lines represent the results calculated with $a = 0.9$ (red), 0.5 (green), and 0 (blue), respectively. The different type lines represent the spectra observed at different angles, i.e., $\theta_{\text{obs}} = 60^\circ$ (dash-dotted), 30° (dashed), 10° (dotted).

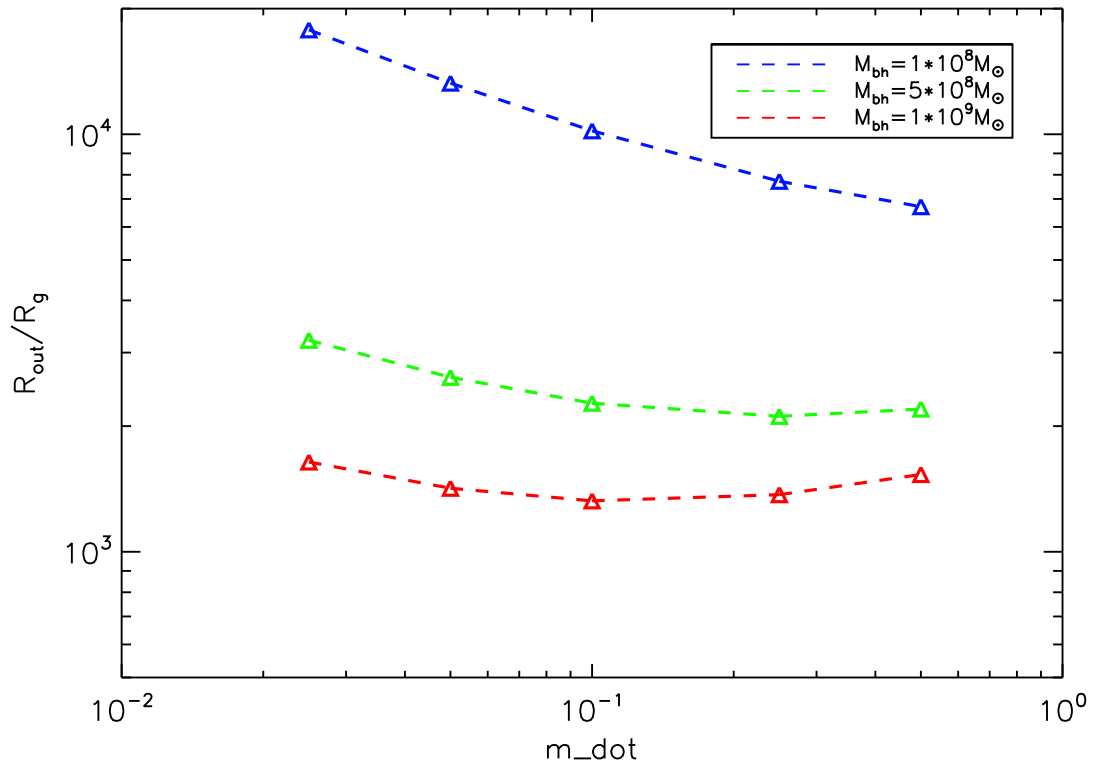


Fig. 6.— The outer radii of the accretion disks as functions of accretion rate \dot{m} for different black hole mass M_{bh} with $\tau_{r\varphi} = \alpha \sqrt{P_{\text{gas}} P_{\text{tot}}}$ (blue: $M_{\text{bh}} = 10^8 M_\odot$, green: $M_{\text{bh}} = 5 \times 10^8 M_\odot$, red: $M_{\text{bh}} = 10^9 M_\odot$).

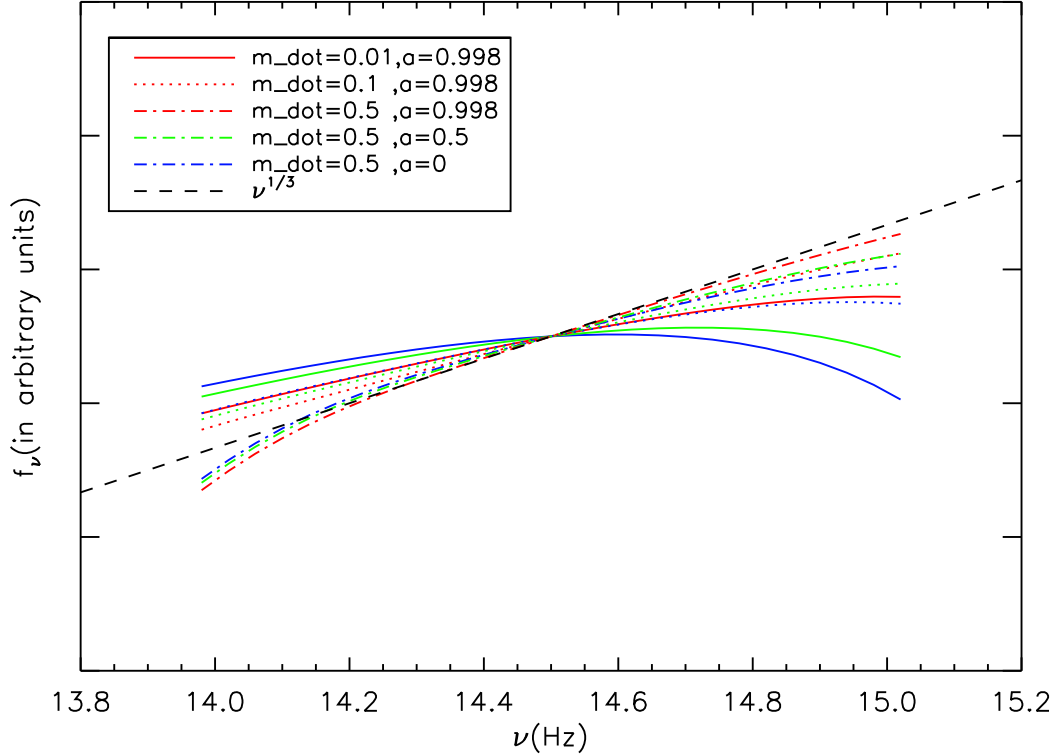


Fig. 7.— The spectral shapes of the disk-corona systems in the near IR/optical wavebands with $\tau_{r\varphi} = \alpha \sqrt{P_{\text{gas}} P_{\text{tot}}}$. The colored lines represent the model calculations with different values of black hole spin parameter, i.e., $a = 0$ (blue), 0.5 (green), and 0.998 (red). The different type lines represent the results calculated with different values of accretion rate, i.e., $\dot{m} = 0.01$ (solid), 0.1 (dotted), and 0.5 (dash-dotted). The dashed line represents $f_\nu \propto \nu^{1/3}$, expected by the standard thin disk model.